



Generalized stress intensity factors in the interaction between two fibers in matrix

NAO-AKI NODA¹, YASUSHI TAKASE¹ and MENGCHENG CHEN²

¹*Department of Mechanical Engineering, Kyushu Institute of Technology, Kitakyushu 804-8550, Japan; e-mail: noda@mech.kyutech.ac.jp*

²*Department of Mechanical Engineering, East China Jiaotong University, Nanchang 8330013, China*

Received 24 November 1998; accepted in revised form 2 September 1999

Abstract. To evaluate the mechanical strength of fiber reinforced composites it is necessary to consider singular stresses at the end of fibers because they cause crack initiation, propagation, and final failure. The singular stress is expressed by generalized stress intensity factors defined at the corner of fibers. As a 2D model an interaction between rectangular inclusions under longitudinal tension is treated in this paper. The body force method is used to formulate the problem as a system of singular integral equations with Cauchy-type or logarithmic-type singularities, where the unknown functions are the densities of body forces distributed in infinite plates having the same elastic constants as those of the matrix and inclusions. In order to analyze the problem accurately, the unknown functions are expressed as piecewise smooth functions using two types of fundamental densities and power series, where the fundamental densities are chosen to represent the symmetric stress singularity of $1/r^{1-\lambda_1}$ and the skew-symmetric stress singularity of $1/r^{1-\lambda_2}$. Then, generalized stress intensity factors at the end of inclusions are systematically calculated for various locations, spacings and elastic modulus of two rectangular inclusions in a plate subjected to longitudinal tension.

Keywords: Elasticity, composite material, fracture mechanics, fiber, generalized stress intensity factor, end effect, interaction, rectangular inclusions.

1. Introduction

To evaluate the mechanical strength of fiber reinforced composites it is necessary to consider singular stresses at the end of fibers because they cause crack initiation, propagation, and final failure. Recently, the singular stress is found to be controlled by generalized stress intensity factors defined at the corner of fibers (Chen and Nisitani, 1993). Chen (1992) has analyzed a rectangular inclusion as a 2D model of fibers using the body force method (Nisitani, 1967). Then, he has discussed the magnitude of the singular stress around the corner of fibers in detail. In addition, Noda et al. (1998a) have considered numerical solutions of the singular integral equations of the body force method when two rectangular inclusions located symmetrically to y axis are under longitudinal tension. In this analysis the unknown functions are approximated as piecewise smooth functions using ‘fundamental densities’ and power series; then, the method is found to yield rapidly converging results for various geometrical conditions. However, it is necessary to treat more general problems to discuss the interaction of fibers in composites. This paper, therefore, deals with two rectangular inclusions, one of which is located at origin and the other of which is located at a point (x, y) as shown in Fig. 1. Then, the interaction will be clarified with varying the location, shape, spacing, and the elastic ratios of inclusions. The discussion will be useful for considering the mechanical strength of fiber reinforced composites.

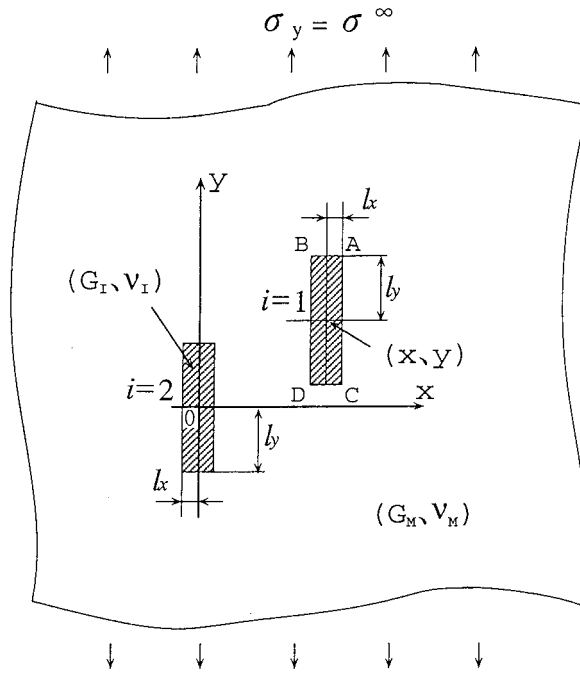


Figure 1. Two rectangular inclusions in an infinite plate.

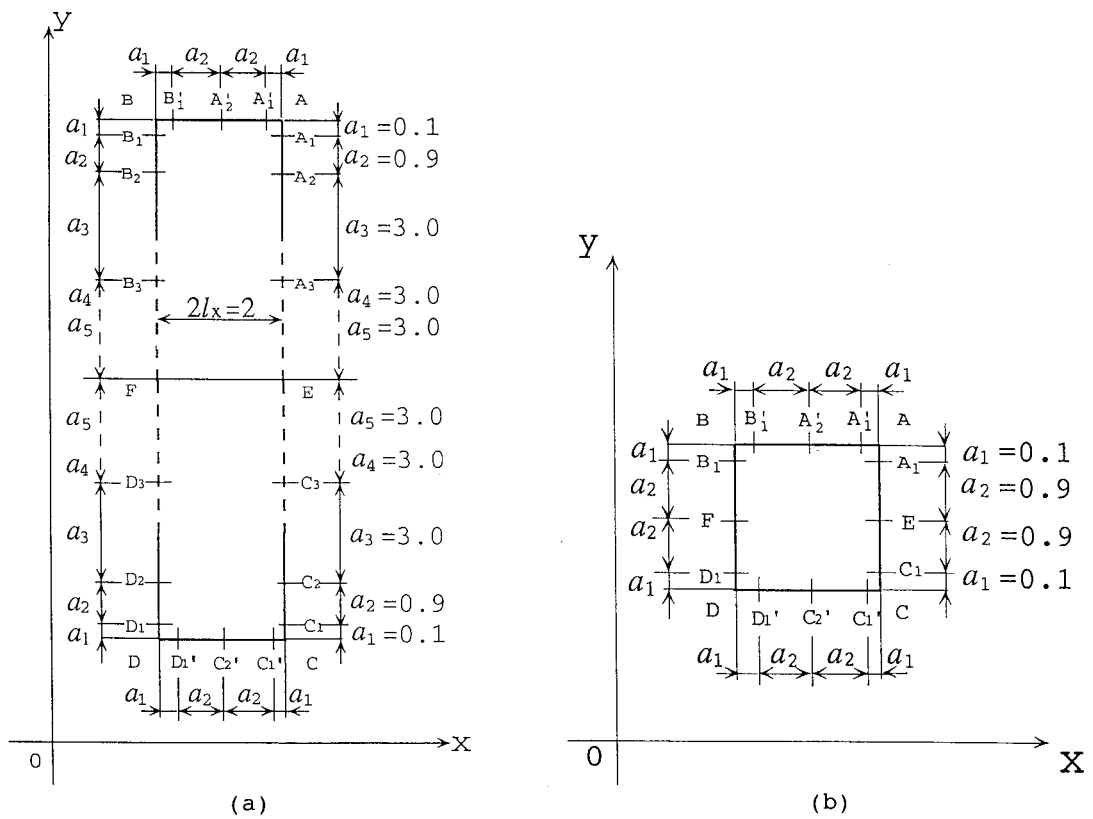


Figure 2. Boundary division for Equations (3), (4), (a) rectangular inclusions, (b) square inclusions.

Table 1. Convergence of F_{I,λ_1} and F_{II,λ_2} at the corner D when the center of inclusion 1 is on O_3 in Fig. 6 ($l_x = \frac{1}{3}$, $G_I/G_M = 10^2$, plane strain $\nu_I = \nu_M = 0.3$)

| M | $F_{I,\lambda_1} (\lambda_1 = 0.7632349)$ | | | $F_{II,\lambda_2} (\lambda_2 = 0.6218440)$ | | |
|---|---|-----------------|---------|--|--------------------|---------|
| | From $W_t^I(0)$ | From $W_n^I(0)$ | Average | From $W_t^{II}(0)$ | From $W_n^{II}(0)$ | Average |
| 3 | 0.6963 | 0.6833 | 0.6898 | 1.0437 | 1.0436 | 1.0437 |
| 4 | 0.6854 | 0.6756 | 0.6805 | 1.0335 | 1.0335 | 1.0335 |
| 5 | 0.6945 | 0.6863 | 0.6904 | 1.0435 | 1.0434 | 1.0435 |
| 6 | 0.6839 | 0.6869 | 0.6904 | 1.0434 | 1.0434 | 1.0434 |

Table 2. Convergence of F_{I,λ_1} and F_{II,λ_2} at the corner D when the center of inclusion 1 is on O_4 in Fig. 6 ($l_x = \frac{1}{2}$, $G_I/G_M = 10^1$, plane strain $\nu_I = \nu_M = 0.3$)

| M | $F_{I,\lambda_1} (\lambda_1 = 0.7981112)$ | | | $F_{II,\lambda_2} (\lambda_2 = 0.78565474)$ | | |
|---|---|-----------------|---------|---|--------------------|---------|
| | From $W_t^I(0)$ | From $W_n^I(0)$ | Average | From $W_t^{II}(0)$ | From $W_n^{II}(0)$ | Average |
| 3 | 0.5261 | 0.5053 | 0.5157 | 0.9884 | 0.9881 | 0.9883 |
| 4 | 0.5243 | 0.5076 | 0.5159 | 0.9887 | 0.9886 | 0.9886 |
| 5 | 0.5231 | 0.5087 | 0.5159 | 0.9885 | 0.9884 | 0.9884 |

2. Numerical solution of singular integral equations of body force method

Consider two rectangular inclusions with the same configuration in an infinite plate as shown in Fig. 1. Here, l_x and l_y are sizes of inclusions, d_x and d_y is a parameter of distance, $\sigma_x^\infty, \sigma_y^\infty, \tau_{xy}^\infty$ are stresses at infinity. Denote the shear modulus and Poisson's ratios of the matrix by G_M and ν_M and the inclusions by G_I and ν_I . The problem can be expressed as a system of singular integral equations (1) and (2), where the unknowns are body forces densities $F_{nM}, F_{tM}, F_{nI}, F_{tI}$, ($i = 1, 2$) distributed in the normal and tangential directions along the

Table 3. Convergence of F_{I,λ_1} and F_{II,λ_2} at the corner D when the center of inclusion 1 is on O_4 in Fig. 6 ($l_x = \frac{2}{3}$, $G_I/G_M = 10^{-5}$, plane strain $\nu_I = \nu_M = 0.3$)

| M | $F_{I,\lambda_1} (\lambda_1 = 0.54448375)$ | | | $F_{II,\lambda_2} (\lambda_2 = 0.90852919)$ | | |
|---|--|-----------------|---------|---|--------------------|---------|
| | From $W_t^I(0)$ | From $W_n^I(0)$ | Average | From $W_t^{II}(0)$ | From $W_n^{II}(0)$ | Average |
| 3 | 0.5165 | 0.5167 | 0.5166 | 1.8491 | 1.8488 | 1.8489 |
| 4 | 0.5167 | 0.5167 | 0.5167 | 1.8496 | 1.8496 | 1.8496 |
| 5 | 0.5163 | 0.5163 | 0.5163 | 1.8497 | 1.8497 | 1.8497 |

imaginary boundary in two infinite plates, ‘M’ and ‘I’ (Noda et al., 1996). Here, the infinite plates ‘M’ has the same elastic constants as those of the matrix, and the infinite plate ‘I’ has the same elastic constants as those of the inclusions.

$$\begin{aligned}
& -\frac{1}{2}F_{nM}(s_i) - \frac{1}{2}F_{nI}(s_i) + \sum_{k=1}^2 \left[\int_{L_k} h_{nn}^{F_{nM}}(r_k, s_i) F_{nM}(r_k) \, dr_k \right. \\
& + \int_{L_k} h_{nn}^{F_{tM}}(r_k, s_i) F_{tM}(r_k) \, dr_k - \int_{L_k} h_{nn}^{F_{nI}}(r_k, s_i) F_{nI}(r_k) \, dr_k \\
& \left. - \int_{L_k} h_{nn}^{F_{tI}}(r_k, s_i) F_{tI}(r_k) \, dr_k \right] = -\sigma_{nM}^\infty(s_i) + \sigma_{nI}^\infty(s_i), \\
& -\frac{1}{2}F_{tM}(s_i) - \frac{1}{2}F_{tI}(s_i) + \sum_{k=1}^2 \left[\int_{L_k} h_{nt}^{F_{nM}}(r_k, s_i) F_{nM}(r_k) \, dr_k \right. \\
& + \int_{L_k} h_{nt}^{F_{tM}}(r_k, s_i) F_{tM}(r_k) \, dr_k - \int_{L_k} h_{nt}^{F_{nI}}(r_k, s_i) F_{nI}(r_k) \, dr_k \\
& \left. - \int_{L_k} h_{nt}^{F_{tI}}(r_k, s_i) F_{tI}(r_k) \, dr_k \right] = -\tau_{ntM}^\infty(s_i) + \tau_{ntI}^\infty(s_i) \quad (i = 1, 2),
\end{aligned} \tag{1}$$

$$\begin{aligned}
& \sum_{k=1}^2 \left[\int_{L_k} h_u^{F_{nM}}(r_k, s_i) F_{nM}(r_k) \, dr_k + \int_{L_k} h_u^{F_{tM}}(r_k, s_i) F_{tM}(r_k) \, dr_k \right. \\
& \left. - \int_{L_k} h_u^{F_{nI}}(r_k, s_i) F_{nI}(r_k) \, dr_k - \int_{L_k} h_u^{F_{tI}}(r_k, s_i) F_{tI}(r_k) \, dr_k \right] \\
& = -u_{M,i}^\infty + u_{I,i}^\infty, \\
& \sum_{k=1}^2 \left[\int_{L_k} h_v^{F_{nM}}(r_k, s_i) F_{nM}(r_k) \, dr_k + \int_{L_k} h_v^{F_{tM}}(r_k, s_i) F_{tM}(r_k) \, dr_k \right. \\
& \left. - \int_{L_k} h_v^{F_{nI}}(r_k, s_i) F_{nI}(r_k) \, dr_k - \int_{L_k} h_v^{F_{tI}}(r_k, s_i) F_{tI}(r_k) \, dr_k \right] \\
& = -v_{M,i}^\infty + v_{I,i}^\infty \quad (i = 1, 2)
\end{aligned} \tag{2}$$

Equations (1) and (2) enforce the boundary conditions along the interface, that is, $\sigma_{nM} - \sigma_{nI} = 0$, $\tau_{ntM} - \tau_{ntI} = 0$, $u_M - u_I = 0$, $v_M - v_I = 0$. Here, (u_M, v_M) and $(\sigma_{nM}, \tau_{ntM})$ are the displacements and tractions, respectively, on the prospective boundary of rectangular holes in the infinite plate ‘M’. On the other hand, (u_I, v_I) and $(\sigma_{nI}, \tau_{ntI})$ are the displacements and tractions, respectively, on the prospective boundary of rectangular inclusions in the infinite plate ‘I’. In eqn. (1) and (2), $\sum_{k=1}^2$ denotes the sum total about the prospective boundary of each rectangular holes and inclusions, and \int_{L_k} means integrating the body forces on the boundary of the k th rectangular hole in the plate M, or the k th inclusion in the plate ‘I’.

The notations $\sigma_{nM}^\infty(s_i)$ and $\tau_{ntM}^\infty(s_i)$ denote normal and shear stresses, respectively, appearing at the point s_i in plate ‘M’. We assume the infinite plate ‘I’ is also under the stresses σ_{xI}^∞

Table 4. Results for a single rectangular inclusion (Plane strain $\nu_I = \nu_M = 0.3$)

| L/D | G_I/G_M | | F_{II,λ_2} | | | | | | | | | |
|--------------------|-----------|-----------|--------------------|-------|-------|--------|-----------|-----------|-----------|-------|-------|--------|
| | 10^{-5} | 10^{-2} | 10^{-1} | 2 | 10 | 10^2 | 10^{-5} | 10^{-2} | 10^{-1} | 2 | 10 | 10^2 |
| $10^{0.0} = 1.0$ | 0.505 | 0.476 | 0.327 | 0.192 | 0.213 | 0.224 | 2.139 | 2.159 | 2.361 | 2.835 | 0.493 | 0.385 |
| $10^{0.5} = 3.162$ | 0.540 | 0.511 | 0.359 | 0.240 | 0.359 | 0.413 | 2.044 | 2.060 | 2.233 | 3.072 | 0.707 | 0.646 |
| $10^{1.0} = 10.0$ | 0.513 | 0.489 | 0.351 | 0.258 | 0.495 | 0.673 | 1.968 | 1.979 | 2.135 | 3.262 | 0.944 | 1.018 |
| $10^{1.5} = 31.62$ | 0.502 | 0.484 | 0.348 | 0.264 | 0.593 | 1.064 | 1.938 | 1.944 | 2.099 | 3.338 | 1.137 | 1.619 |
| $10^{2.0} = 100.0$ | 0.498 | 0.484 | 0.347 | 0.265 | 0.635 | 1.544 | 1.940 | 1.930 | 2.083 | 3.362 | 1.224 | 2.377 |
| $10^{2.5} = 316.2$ | 0.497 | 0.483 | 0.346 | 0.266 | 0.649 | 1.893 | 1.924 | 1.931 | 2.084 | 3.369 | 1.248 | 2.933 |
| $10^{3.0} = 1000$ | 0.493 | 0.483 | 0.346 | 0.266 | 0.651 | 1.950 | 1.924 | 1.926 | 2.081 | 3.371 | 1.255 | 2.977 |

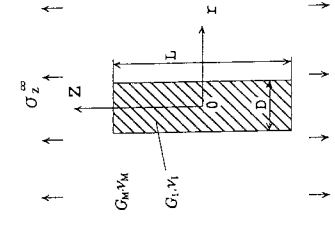


Table 5. Results for a single cylindrical inclusion

| L/D | G_I/G_M | | F_{II,λ_2} | | | | | | | | | |
|--------------------|-----------|-----------|--------------------|-------|-------|--------|-----------|-----------|-----------|-------|-------|--------|
| | 10^{-5} | 10^{-2} | 10^{-1} | 2 | 10 | 10^2 | 10^{-5} | 10^{-2} | 10^{-1} | 2 | 10 | 10^2 |
| $10^{0.0} = 1.0$ | 0.391 | 0.373 | 0.280 | 0.218 | 0.291 | 0.320 | 1.678 | 1.703 | 1.952 | 3.038 | 0.629 | 0.546 |
| $10^{0.5} = 3.162$ | 0.382 | 0.366 | 0.278 | 0.249 | 0.437 | 0.659 | 1.616 | 1.641 | 1.877 | 3.246 | 0.891 | 0.959 |
| $10^{1.0} = 10.0$ | 0.379 | 0.363 | 0.277 | 0.255 | 0.599 | 1.298 | 1.604 | 1.627 | 1.862 | 3.302 | 1.087 | 1.816 |
| $10^{1.5} = 31.62$ | 0.379 | 0.363 | 0.276 | 0.255 | 0.618 | 1.982 | 1.602 | 1.623 | 1.860 | 3.308 | 1.120 | 2.692 |
| $10^{2.0} = 100.0$ | 0.379 | 0.363 | 0.276 | 0.255 | 0.618 | 2.113 | 1.600 | 1.624 | 1.860 | 3.308 | 1.121 | 2.891 |
| $10^{2.5} = 316.2$ | 0.379 | 0.363 | 0.276 | 0.255 | 0.618 | 2.099 | 1.600 | 1.624 | 1.859 | 3.308 | 1.119 | 2.891 |
| $10^{3.0} = 1000$ | 0.379 | 0.362 | 0.276 | 0.255 | 0.618 | 2.118 | 1.600 | 1.631 | 1.860 | 3.308 | 1.119 | 2.892 |

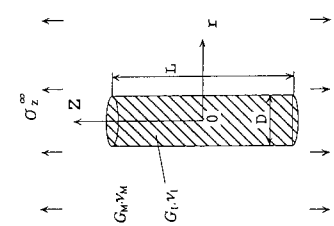


Table 6. Results for two square inclusions ($G_I/G_M = 10^2$, plane strain $\nu_I = \nu_M = 0.3$)

| G_I/G_M | I_x/d_x | | $F_{I,\lambda_1} (F_{I,\lambda_1}/F_{I,\lambda_1} _{I_x \rightarrow 0})$ | | | | | $F_{II,\lambda_2} (F_{II,\lambda_2}/F_{II,\lambda_2} _{I_x \rightarrow 0})$ | | | | | |
|---|-----------------|---------------|--|----------------|----------------|----------------|----------------|---|----------------|----------------|----------------|----------------|----------------|
| | | | O ₁ | O ₂ | O ₃ | O ₄ | O ₅ | O ₁ | O ₂ | O ₃ | O ₄ | O ₅ | |
| 10^2 $\lambda_1 = 0.7632349$ $\lambda_2 = 0.6218440$ $\alpha = -0.9801980$ $\beta = -0.2800566$ | $\rightarrow 0$ | A-D | 0.224 | 0.224 | 0.224 | 0.224 | 0.224 | ± 0.385 | ± 0.385 | ± 0.385 | ± 0.385 | ± 0.385 | |
| | | | (1.000) | (1.000) | (1.000) | (1.000) | (1.000) | (1.000) | (1.000) | (1.000) | (1.000) | (1.000) | |
| | | $\frac{1}{3}$ | A | 0.212 | 0.216 | 0.226 | 0.237 | 0.237 | 0.395 | 0.377 | 0.377 | 0.380 | 0.404 |
| | | | | (0.946) | (0.964) | (1.009) | (1.058) | (1.058) | (1.026) | (0.979) | (0.979) | (0.987) | (1.049) |
| | B | | 0.220 | 0.225 | 0.218 | 0.218 | 0.237 | -0.390 | -0.370 | -0.379 | -0.395 | -0.404 | |
| | | | (0.982) | (1.004) | (0.973) | (0.973) | (1.058) | (1.013) | (0.961) | (0.984) | (1.026) | (1.049) | |
| | | C | 0.212 | 0.226 | 0.224 | 0.213 | 0.222 | -0.395 | -0.389 | -0.377 | -0.373 | -0.403 | |
| | | | (0.946) | (1.009) | (1.000) | (0.951) | (0.991) | (1.026) | (1.010) | (0.979) | (0.969) | (1.047) | |
| | | D | 0.220 | 0.199 | 0.228 | 0.260 | 0.222 | 0.390 | 0.383 | 0.377 | 0.393 | 0.403 | |
| | | | (0.982) | (0.888) | (1.018) | (1.161) | (0.991) | (1.013) | (0.995) | (0.979) | (1.021) | (1.047) | |
| | $\frac{1}{2}$ | $\frac{1}{3}$ | A | 0.200 | 0.212 | 0.228 | 0.248 | 0.254 | 0.404 | 0.368 | 0.369 | 0.375 | 0.421 |
| | | | | (0.893) | (0.946) | (1.018) | (1.107) | (1.134) | (1.049) | (0.956) | (0.958) | (0.974) | (1.094) |
| B | | | 0.222 | 0.220 | 0.212 | 0.221 | 0.254 | -0.372 | -0.351 | -0.377 | -0.418 | -0.421 | |
| | | | (0.991) | (0.982) | (0.946) | (0.987) | (1.134) | (0.966) | (0.912) | (0.979) | (1.086) | (1.094) | |
| | | C | 0.200 | 0.222 | 0.225 | 0.203 | 0.207 | -0.404 | -0.401 | -0.372 | -0.354 | -0.405 | |
| | | | (0.893) | (0.991) | (1.004) | (0.906) | (0.924) | (1.049) | (1.042) | (0.966) | (0.919) | (1.052) | |
| | | D | 0.222 | 0.159 | 0.236 | 0.310 | 0.207 | 0.372 | 0.389 | 0.369 | 0.416 | 0.405 | |
| | | | (0.991) | (0.710) | (1.054) | (1.384) | (0.924) | (0.966) | (1.010) | (0.958) | (1.081) | (1.052) | |
| $\frac{2}{3}$ | | A | 0.189 | 0.209 | 0.231 | 0.259 | 0.273 | 0.411 | 0.356 | 0.359 | 0.368 | 0.441 | |
| | | | (0.844) | (0.933) | (1.031) | (1.156) | (1.219) | (1.068) | (0.925) | (0.932) | (0.956) | (1.145) | |
| | | B | 0.212 | 0.211 | 0.206 | 0.235 | 0.273 | -0.313 | -0.332 | -0.382 | -0.456 | -0.441 | |
| | | | (0.946) | (0.942) | (0.920) | (1.049) | (1.219) | (0.813) | (0.862) | (0.992) | (1.184) | (1.145) | |
| | C | 0.189 | 0.210 | 0.225 | 0.191 | 0.188 | -0.411 | -0.422 | -0.368 | -0.323 | -0.371 | | |
| | | (0.844) | (0.938) | (1.004) | (0.853) | (0.839) | (1.068) | (1.096) | (0.956) | (0.839) | (0.964) | | |
| | D | 0.212 | 0.125 | 0.257 | 0.355 | 0.188 | 0.313 | 0.395 | 0.369 | 0.453 | 0.371 | | |
| | | (0.946) | (0.558) | (1.147) | (1.585) | (0.839) | (0.813) | (1.026) | (0.958) | (1.177) | (0.964) | | |

σ_{yI}^∞ τ_{xyI}^∞ , which produce $\sigma_{nI}^\infty(s_I)$ and $\tau_{nI}^\infty(s_i)$ in Equation (1) at the prospective boundary for inclusions. As an example, the notation $h_{nm}^{F_{nm}}(r_k, s_i)$ denotes the normal stress induced at the collocation point s_i on the imaginary boundary of the i th rectangular hole when the body force with unit density is acting at the point r_k on the prospective boundary of the k th rectangular hole.

Around corners A, B, C, D it is known that the body forces acting in the normal and tangential directions F_n and F_t should be expressed as two types, that is, symmetric mode I type $r_A^{\lambda_1-1}$ and skew-symmetric mode II type $r_A^{\lambda_2-1}$ to the bisector of the corners (Chen, 1992). Here, r_A is a distance measured from the corner A, and the eigenvalues λ_1 and λ_2 are given as the roots of eigenequations (Bogy and Wang, 1971; Chen and Nisitani, 1993). Figure 2 illustrates boundary divisions for numerical solution of Equations (1) and (2). In the numerical solutions for elliptical inclusions, we do not have to divide the boundaries because

Table 7. Results for two square inclusions ($G_I/G_M = 10^1$, plane strain $\nu_I = \nu_M = 0.3$)

| G_I/G_M | I_x/d_x | | $F_{I,\lambda_1} (F_{I,\lambda_1}/F_{I,\lambda_1} _{I_x \rightarrow 0})$ | | | | | $F_{II,\lambda_2} (F_{II,\lambda_2}/F_{II,\lambda_2} _{I_x \rightarrow 0})$ | | | | |
|---|-----------------|------------------|--|------------------|----------------------------------|----------------------------------|------------------|---|------------------------|----------------------------------|----------------------------------|-----------------------------------|
| | | | O ₁ | O ₂ | O ₃ | O ₄ | O ₅ | O ₁ | O ₂ | O ₃ | O ₄ | O ₅ |
| 10^1 $\lambda_1 = 0.7981112$ $\lambda_2 = 0.7856547$ $\alpha = 0.8181818$ $\beta = 0.2337662$ | $\rightarrow 0$ | A-D | 0.213 (1.000) | 0.213 (1.000) | 0.213 (1.000) | 0.213 (1.000) | 0.213 (1.000) | ± 0.493 (1.000) | ± 0.493 (1.000) | ± 0.493 (1.000) | ± 0.493 (1.000) | ± 0.493 (1.000) |
| | $\frac{1}{3}$ | A | 0.204 (0.958) | 0.208 (0.977) | 0.215 (1.009) | 0.224 (1.052) | 0.224 (1.052) | 0.503 (1.020) | 0.486 (0.986) | 0.486 (0.986) | 0.489 (0.992) | 0.512 (1.039) |
| | | B | 0.211 (0.991) | 0.214 (1.005) | 0.209 (0.981) | 0.209 (0.981) | 0.224 (1.052) | -0.499 (1.012) | -0.478 (0.970) | -0.487 (0.988) | -0.504 (1.022) | -0.512 (1.039) |
| | | C | 0.204 (0.958) | 0.214 (1.005) | 0.214 (1.005) | 0.205 (0.962) | 0.211 (0.991) | -0.503 (1.020) | -0.961 (0.994) | -0.485 (0.984) | -0.482 (0.978) | -0.514 (1.043) |
| | | D | 0.211 (0.991) | 0.194 (0.911) | 0.217 (1.019) | 0.240 (1.127) | 0.211 (0.991) | 0.499 (1.012) | 0.486 (0.986) | 0.484 (0.982) | 0.500 (1.014) | 0.514 (1.043) |
| | $\frac{1}{2}$ | A | 0.195 (0.915) | 0.204 (0.958) | 0.217 (1.019) | 0.233 (1.094) | 0.238 (1.117) | 0.510 (1.034) | 0.477 (0.968) | 0.477 (0.968) | 0.484 (0.982) | 0.529 (1.073) |
| | | B | 0.213 (1.000) | 0.210 (0.986) | 0.204 (0.958) | 0.211 (0.991) | 0.238 (1.117) | -0.481 (0.976) | -0.458 (0.929) | -0.486 (0.986) | -0.526 (1.067) | -0.529 (1.073) |
| | | C | 0.195 (0.915) | 0.213 (1.000) | 0.215 (1.009) | 0.196 (0.920) | 0.198 (0.930) | -0.510 (1.034) | -0.512 (1.039) | -0.479 (0.972) | -0.461 (0.935) | -0.518 (1.051) |
| | | D | 0.213 (1.000) | 0.164 (0.770) | 0.224 (1.052) | 0.282 (1.324) | 0.198 (0.930) | 0.481 (0.976) | 0.495 (1.004) | 0.474 (0.961) | 0.529 (1.073) | 0.518 (1.051) |
| | $\frac{2}{3}$ | A | 0.185 (0.869) | 0.201 (0.944) | 0.220 (1.033) | 0.242 (1.136) | 0.253 (1.188) | 0.517 (1.049) | 0.466 (0.945) | 0.468 (0.949) | 0.477 (0.968) | 0.547 (1.110) |
| | | B | 0.207 (0.972) | 0.200 (0.939) | 0.199 (0.934) | 0.221 (1.038) | 0.253 (1.188) | -0.421 (0.854) | -0.441 (0.895) | -0.492 (0.998) | -0.561 (1.138) | -0.547 (1.110) |
| | | C | 0.185 (0.869) | 0.204 (0.958) | 0.216 (1.014) | 0.192 (0.901) | 0.179 (0.840) | -0.517 (1.049) | -0.527 (1.069) | -0.474 (0.961) | -0.432 (0.876) | -0.485 (0.984) |
| | D | 0.207 (0.972) | 0.135 (0.634) | 0.241 (1.131) | 0.320 (1.502) | 0.179 (0.840) | 0.421 (0.854) | 0.502 (1.018) | 0.465 (0.943) | 0.577 (1.170) | 0.485 (0.984) | |

the ‘fundamental densities’ to express an elliptical inclusion exactly are available (Noda and Matsuo, 1998). On the other hand, the boundary division is introduced for rectangular inclusion problems because in this problem the fundamental densities are only useful near the corner. The body force densities distributed in the regions $B_2 - B - A - A_2$ and $D_2 - D - C - C_2$ are expressed as follows using fundamental densities $r_A^{\lambda_1-1}$, $r_A^{\lambda_2-1}$ and weight functions $W_{nM}^I \sim W_{iM}^{II}$. Here, the following expressions are shown by taking an example for corner A. Similar expressions of Equations (3) and (4) can be given for corners B, C, D.

Table 8. Results for two square inclusions ($G_I/G_M = 10^{-1}$, plane strain $\nu_I = \nu_M = 0.3$)

| G_I/G_M | I_x/d_x | | $F_{I,\lambda_1} (F_{I,\lambda_1}/F_{I,\lambda_1} _{I_x \rightarrow 0})$ | | | | | $F_{II,\lambda_2} (F_{II,\lambda_2}/F_{II,\lambda_2} _{I_x \rightarrow 0})$ | | | | |
|-------------------------|-----------------|-----|--|----------------|----------------|----------------|----------------|---|----------------|----------------|----------------|----------------|
| | | | O ₁ | O ₂ | O ₃ | O ₄ | O ₅ | O ₁ | O ₂ | O ₃ | O ₄ | O ₅ |
| 10^{-1} | $\rightarrow 0$ | A–D | 0.327 | 0.327 | 0.327 | 0.327 | 0.327 | ± 2.361 | ± 2.361 | ± 2.361 | ± 2.361 | ± 2.361 |
| $\lambda_1 = 0.6601418$ | | | (1.000) | (1.000) | (1.000) | (1.000) | (1.000) | (1.000) | (1.000) | (1.000) | (1.000) | (1.000) |
| $\lambda_2 = 0.9355639$ | $\frac{1}{3}$ | A | 0.335 | 0.326 | 0.333 | 0.343 | 0.324 | 2.350 | 2.406 | 2.399 | 2.375 | 2.265 |
| $\alpha = 0.8181818$ | | | (1.024) | (0.997) | (1.018) | (1.049) | (0.991) | (0.995) | (1.019) | (1.016) | (1.006) | (0.959) |
| $\beta = 0.2337662$ | | B | 0.355 | 0.333 | 0.313 | 0.294 | 0.324 | 2.332 | 2.465 | 2.397 | 2.295 | 2.265 |
| | | | (1.086) | (1.018) | (0.957) | (0.899) | (0.991) | (0.988) | (1.044) | (1.015) | (0.972) | (0.959) |
| | | C | 0.335 | 0.346 | 0.326 | 0.298 | 0.288 | 2.350 | 2.340 | 2.412 | 2.415 | 2.161 |
| | | | (1.024) | (1.058) | (0.997) | (0.911) | (0.881) | (0.995) | (0.991) | (1.022) | (1.023) | (0.915) |
| | | D | 0.355 | 0.321 | 0.335 | 0.356 | 0.288 | 2.332 | 2.433 | 2.452 | 2.284 | 2.161 |
| | | | (1.086) | (0.982) | (1.024) | (1.089) | (0.881) | (0.988) | (1.030) | (1.039) | (0.967) | (0.915) |
| | $\frac{1}{2}$ | A | 0.343 | 0.329 | 0.338 | 0.356 | 0.326 | 2.371 | 2.448 | 2.432 | 2.399 | 2.226 |
| | | | (1.049) | (1.006) | (1.034) | (1.089) | (0.997) | (1.004) | (1.037) | (1.030) | (1.016) | (0.943) |
| | | B | 0.388 | 0.320 | 0.290 | 0.263 | 0.326 | 2.407 | 2.588 | 2.405 | 2.189 | 2.226 |
| | | | (1.187) | (0.979) | (0.887) | (0.804) | (0.997) | (1.019) | (1.096) | (1.019) | (0.927) | (0.943) |
| | | C | 0.343 | 0.366 | 0.337 | 0.291 | 0.226 | 2.371 | 2.360 | 2.460 | 2.585 | 2.045 |
| | | | (1.049) | (1.119) | (1.031) | (0.890) | (0.691) | (1.004) | (1.000) | (1.042) | (1.095) | (0.866) |
| | | D | 0.388 | 0.327 | 0.350 | 0.397 | 0.226 | 2.407 | 2.494 | 2.626 | 2.158 | 2.045 |
| | | | (1.187) | (1.000) | (1.070) | (1.214) | (0.691) | (1.019) | (1.056) | (1.112) | (0.914) | (0.866) |
| | $\frac{2}{3}$ | A | 0.355 | 0.337 | 0.346 | 0.370 | 0.328 | 2.411 | 2.491 | 2.465 | 2.430 | 2.217 |
| | | | (1.086) | (1.031) | (1.058) | (1.131) | (1.003) | (1.021) | (1.055) | (1.044) | (1.029) | (0.939) |
| | | B | 0.410 | 0.277 | 0.255 | 0.229 | 0.328 | 2.572 | 2.661 | 2.365 | 2.044 | 2.217 |
| | | | (1.254) | (0.847) | (0.780) | (0.700) | (1.003) | (1.089) | (1.127) | (1.002) | (0.866) | (0.939) |
| | | C | 0.355 | 0.388 | 0.357 | 0.314 | 0.159 | 2.411 | 2.363 | 2.478 | 2.693 | 2.036 |
| | | | (1.086) | (1.187) | (1.092) | (0.960) | (0.486) | (1.021) | (1.001) | (1.050) | (1.141) | (0.862) |
| | | D | 0.410 | 0.375 | 0.375 | 0.433 | 0.159 | 2.572 | 2.630 | 2.969 | 1.690 | 2.036 |
| | | | (1.254) | (1.147) | (1.147) | (1.324) | (0.486) | (1.089) | (1.114) | (1.258) | (0.716) | (0.862) |

$$\begin{aligned}
F_{nM}(r_A) &= F_{nM}^I(r_A) + F_{nM}^{II}(r_A) = W_{nM}^I(r_A)r_A^{\lambda_1-1} + W_{nM}^{II}(r_A)r_A^{\lambda_2-1}, \\
F_{tM}(r_A) &= F_{tM}^I(r_A) + F_{tM}^{II}(r_A) = W_{tM}^I(r_A)r_A^{\lambda_1-1} + W_{tM}^{II}(r_A)r_A^{\lambda_2-1}, \\
F_{nI}(r_A) &= F_{nI}^I(r_A) + F_{nI}^{II}(r_A) = W_{nI}^I(r_A)r_A^{\lambda_1-1} + W_{nI}^{II}(r_A)r_A^{\lambda_2-1}, \\
F_{tI}(r_A) &= F_{tI}^I(r_A) + F_{tI}^{II}(r_A) = W_{tI}^I(r_A)r_A^{\lambda_1-1} + W_{tI}^{II}(r_A)r_A^{\lambda_2-1},
\end{aligned} \tag{3}$$

Table 9. Results for two square inclusions ($G_I/G_M = 10^{-5}$, plane strain $\nu_I = \nu_M = 0.3$)

| G_I/G_M | I_x/d_x | | $F_{I,\lambda_1} (F_{I,\lambda_1}/F_{I,\lambda_1} _{I_x \rightarrow 0})$ | | | | | $F_{II,\lambda_2} (F_{II,\lambda_2}/F_{II,\lambda_2} _{I_x \rightarrow 0})$ | | | | | | |
|---------------|-----------------|-------------------------|--|----------------|----------------|----------------|----------------|---|----------------|----------------|----------------|----------------|---------|---------|
| | | | O ₁ | O ₂ | O ₃ | O ₄ | O ₅ | O ₁ | O ₂ | O ₃ | O ₄ | O ₅ | | |
| 10^{-5} | $\rightarrow 0$ | A-D | 0.505 | 0.505 | 0.505 | 0.505 | 0.505 | ± 2.139 | ± 2.139 | ± 2.139 | ± 2.139 | ± 2.139 | | |
| | | | (1.000) | (1.000) | (1.000) | (1.000) | (1.000) | (1.000) | (1.000) | (1.000) | (1.000) | (1.000) | | |
| | | $\lambda_1 = 0.5444838$ | A | 0.525 | 0.508 | 0.518 | 0.538 | 0.496 | 2.139 | 2.194 | 2.182 | 2.154 | 2.025 | |
| | | | | (1.040) | (1.006) | (1.026) | (1.065) | (0.982) | (1.000) | (1.026) | (1.020) | (1.007) | (0.947) | |
| | | | | B | 0.555 | 0.517 | 0.477 | 0.439 | 0.496 | 2.124 | 2.264 | 2.181 | 2.056 | 2.025 |
| | | | | | (1.099) | (1.024) | (0.945) | (0.869) | (0.982) | (0.993) | (1.058) | (1.020) | (0.961) | (0.947) |
| | | C | 0.525 | 0.541 | 0.503 | 0.447 | 0.433 | 2.139 | 2.158 | 2.208 | 2.243 | 1.885 | | |
| | | | (1.040) | (1.071) | (0.996) | (0.885) | (0.857) | (1.000) | (1.009) | (1.032) | (1.049) | (0.881) | | |
| | | D | 0.555 | 0.502 | 0.525 | 0.564 | 0.433 | 2.124 | 2.224 | 2.253 | 2.080 | 1.885 | | |
| | | | (1.099) | (0.994) | (1.040) | (1.117) | (0.857) | (0.993) | (1.040) | (1.053) | (0.972) | (0.881) | | |
| | | $\frac{1}{3}$ | A | 0.547 | 0.518 | 0.532 | 0.569 | 0.495 | 2.174 | 2.242 | 2.217 | 2.183 | 1.987 | |
| | | | | (1.083) | (1.026) | (1.053) | (1.127) | (0.980) | (1.016) | (1.048) | (1.036) | (1.021) | (0.929) | |
| B | 0.606 | | | 0.496 | 0.435 | 0.374 | 0.495 | 2.228 | 2.412 | 2.189 | 1.921 | 1.987 | | |
| | (1.200) | | | (0.982) | (0.861) | (0.741) | (0.980) | (1.042) | (1.128) | (1.023) | (0.898) | (0.929) | | |
| C | 0.547 | | 0.577 | 0.518 | 0.429 | 0.324 | 2.174 | 2.152 | 2.265 | 2.425 | 1.734 | | | |
| | (1.083) | | (1.143) | (1.026) | (0.850) | (0.642) | (1.016) | (1.006) | (1.059) | (1.134) | (0.811) | | | |
| D | 0.606 | | 0.517 | 0.554 | 0.661 | 0.324 | 2.228 | 2.312 | 2.471 | 1.916 | 1.734 | | | |
| | (1.200) | | (1.024) | (1.097) | (1.309) | (0.642) | (1.042) | (1.081) | (1.155) | (0.896) | (0.811) | | | |
| $\frac{2}{3}$ | A | 0.580 | 0.543 | 0.550 | 0.609 | 0.494 | 2.223 | 2.289 | 2.252 | 2.218 | 1.986 | | | |
| | | (1.149) | (1.075) | (1.089) | (1.206) | (0.978) | (1.039) | (1.070) | (1.053) | (1.037) | (0.928) | | | |
| | B | 0.639 | 0.425 | 0.367 | 0.294 | 0.494 | 2.418 | 2.511 | 2.142 | 1.707 | 1.986 | | | |
| | | (1.265) | (0.842) | (0.727) | (0.582) | (0.978) | (1.130) | (1.174) | (1.001) | (0.798) | (0.928) | | | |
| C | 0.580 | 0.618 | 0.555 | 0.485 | 0.212 | 2.223 | 2.161 | 2.293 | 2.557 | 1.702 | | | | |
| | (1.149) | (1.224) | (1.099) | (0.960) | (0.420) | (1.039) | (1.010) | (1.072) | (1.195) | (0.796) | | | | |
| D | 0.639 | 0.622 | 0.604 | 0.795 | 0.212 | 2.418 | 2.594 | 2.943 | 1.275 | 1.702 | | | | |
| | (1.265) | (1.232) | (1.196) | (1.574) | (0.420) | (1.130) | (1.213) | (1.376) | (0.596) | (0.796) | | | | |

$$\begin{aligned}
 W_{nM}^I(r_A) &= \sum_{n=1}^M a_n r_A^{n-1}, & W_{tM}^I(r_A) &= \sum_{n=1}^M b_n r_A^{n-1}, & W_{nM}^{II}(r_A) &= \sum_{n=1}^M c_n r_A^{n-1}, \\
 W_{tM}^{II}(r_A) &= \sum_{n=1}^M d_n r_A^{n-1}, & W_{nI}^I(r_A) &= \sum_{n=1}^M e_n r_A^{n-1}, & W_{tI}^I(r_A) &= \sum_{n=1}^M f_n r_A^{n-1}, \\
 W_{nI}^{II}(r_A) &= \sum_{n=1}^M g_n r_A^{n-1}, & W_{tI}^{II}(r_A) &= \sum_{n=1}^M h_n r_A^{n-1},
 \end{aligned} \tag{4}$$

Equations (3) and (4) do not include the terms expressing local uniform stretching and shear distortion at the corner A. Therefore the stresses σ_{xI}^∞ , σ_{yI}^∞ , τ_{xyI}^∞ applied in the plate 'I' are decided to express local uniform stretching and shear distortion at the corner A.

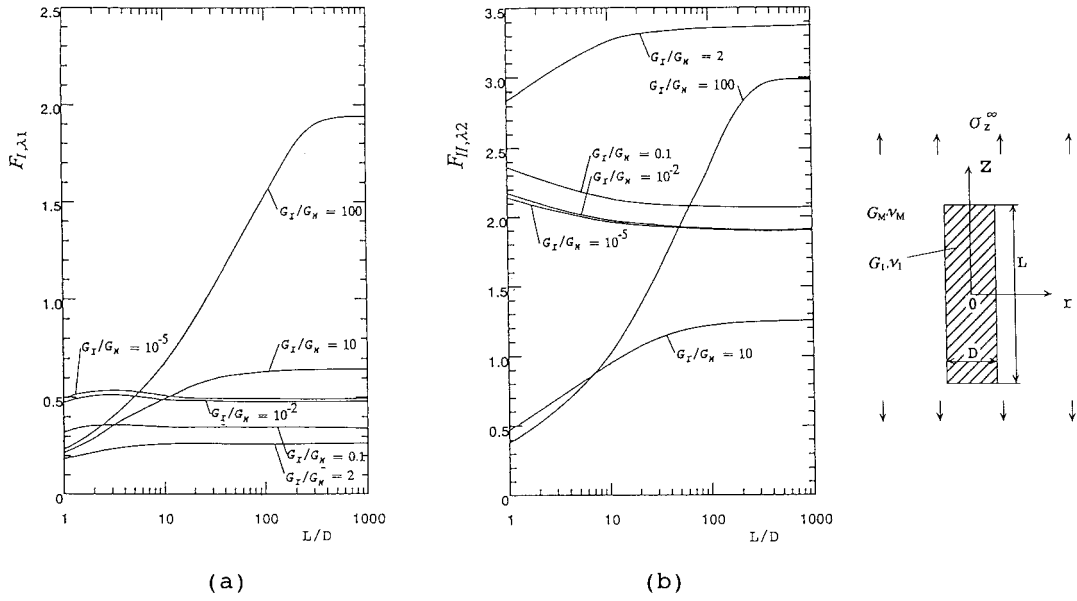


Figure 3. Results for a single rectangular inclusion (a) F_{I,λ_1} (b) F_{II,λ_2} (Plane strain $\nu_I = \nu_M = 0.3$).

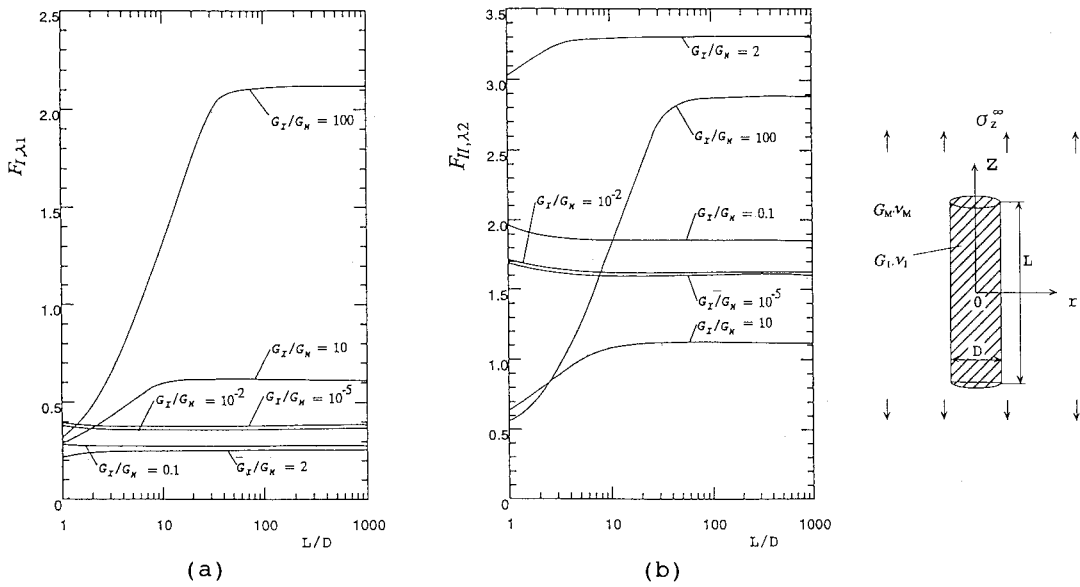


Figure 4. Results for a single cylindrical inclusion, (a) F_{I,λ_1} , (b) F_{II,λ_2} .

Except along the boundaries $B_2 - B - A - A_2$ and $D_2 - D - C - C_2$ in Fig. 2, body forces are simply distributed in the normal and tangential directions without using symmetric and skew-symmetric distributions. On the numerical solution as shown in Equation (3), (4), the singular integral Equations (1), (2) are reduced to algebraic equations for the determination of the unknown coefficients $a_n \sim h_n$. These coefficients are determined from the boundary conditions at suitably chosen collocation points. The generalized stress intensity factors K_{I,λ_1} , K_{II,λ_2} for angular corners can be obtained from the values of $W_n^I(0)$, $W_n^{II}(0)$, $W_t^I(0)$, $W_t^{II}(0)$ at the corner tip (Noda et al., 1996).

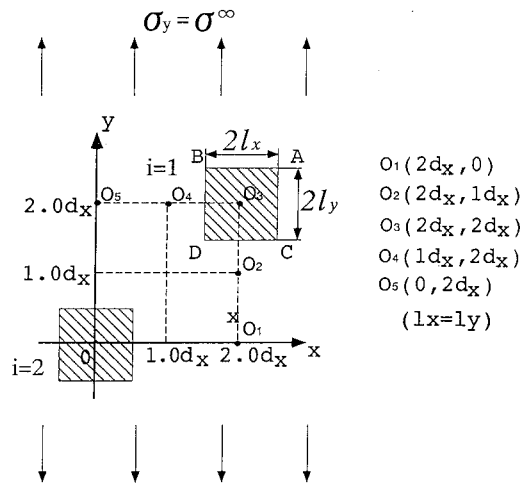


Figure 5. Two square inclusions in an infinite plate (Plane strain $\nu_I = \nu_M = 0.3$).

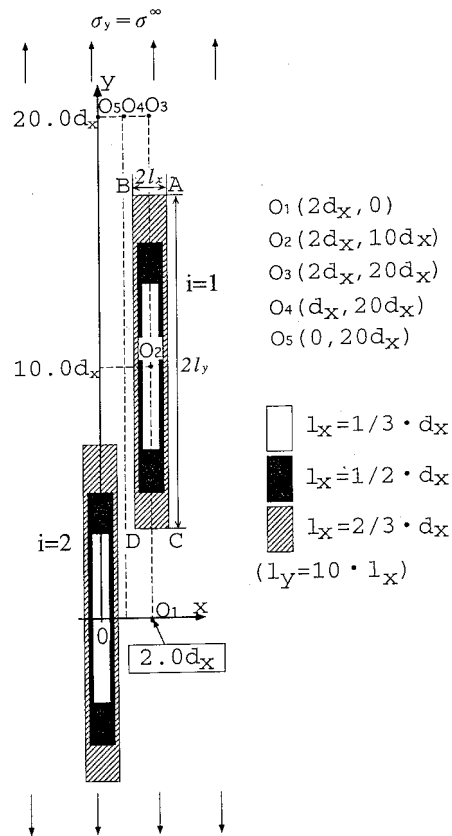


Figure 6. Two rectangular inclusions in an infinite plate (Plane strain $\nu_I = \nu_M = 0.3$).

Table 10. Results for two rectangular inclusions ($G_I/G_M = 10^2$, plane strain $\nu_I = \nu_M = 0.3$)

| G_I/G_M | I_x/d_x | | $F_{I,\lambda_1} (F_{I,\lambda_1}/F_{I,\lambda_1} _{I_x \rightarrow 0})$ | | | | | $F_{II,\lambda_2} (F_{II,\lambda_2}/F_{II,\lambda_2} _{I_x \rightarrow 0})$ | | | | | |
|---|-----------------|------------------|--|----------------------------------|------------------|------------------|------------------|---|----------------------------------|------------------------|------------------------|------------------------|-------------------|
| | | | O ₁ | O ₂ | O ₃ | O ₄ | O ₅ | O ₁ | O ₂ | O ₃ | O ₄ | O ₅ | |
| 10^2 $\lambda_1 = 0.7632349$ $\lambda_2 = 0.6218440$ $\alpha = -0.9801980$ $\beta = -0.2800566$ | $\rightarrow 0$ | A-D | 0.673 (1.000) | 0.673 (1.000) | 0.673 (1.000) | 0.673 (1.000) | 0.673 (1.000) | ± 1.018 (1.000) | ± 1.018 (1.000) | ± 1.018 (1.000) | ± 1.018 (1.000) | ± 1.018 (1.000) | |
| | | $\frac{1}{3}$ | A | 0.593 (0.881) | 0.715 (1.062) | 0.684 (1.016) | 0.684 (1.016) | 0.683 (1.015) | 0.903 (0.887) | 1.075 (1.056) | 1.035 (1.017) | 1.036 (1.017) | 1.035 (1.017) |
| | | | B | 0.529 (0.786) | 0.697 (1.036) | 0.681 (1.012) | 0.682 (1.013) | 0.683 (1.015) | -0.754 (0.741) | -1.066 (1.047) | -1.033 (1.015) | -1.035 (1.016) | -1.035 (1.017) |
| | | | C | 0.593 (0.881) | 0.654 (0.972) | 0.680 (1.010) | 0.683 (1.015) | 0.686 (1.019) | -0.903 (0.887) | -1.046 (1.027) | -1.039 (1.020) | -1.042 (1.023) | -1.043 (1.025) |
| | D | | 0.529 (0.786) | 0.809 (1.202) | 0.690 (1.025) | 0.689 (1.024) | 0.686 (1.019) | 0.754 (0.741) | 1.132 (1.112) | 1.043 (1.025) | 1.044 (1.026) | 1.043 (1.025) | |
| | $\frac{1}{2}$ | A | 0.593 (0.881) | 0.758 (1.126) | 0.698 (1.037) | 0.698 (1.037) | 0.697 (1.036) | 0.912 (0.896) | 1.140 (1.119) | 1.056 (1.037) | 1.057 (1.039) | 1.057 (1.038) | |
| | | B | 0.457 (0.678) | 0.731 (1.086) | 0.692 (1.028) | 0.695 (1.033) | 0.697 (1.036) | -0.654 (0.642) | -1.120 (1.100) | -1.053 (1.034) | -1.055 (1.037) | -1.057 (1.038) | |
| | | C | 0.593 (0.881) | 0.580 (0.862) | 0.688 (1.022) | 0.698 (1.037) | 0.708 (1.052) | -0.912 (0.896) | -0.828 (0.813) | -1.071 (1.052) | -1.081 (1.062) | -1.088 (1.069) | |
| | | D | 0.456 (0.678) | 1.013 (1.505) | 0.724 (1.076) | 0.718 (1.076) | 0.708 (1.052) | 0.654 (0.642) | 1.292 (1.269) | 1.089 (1.069) | 1.091 (1.072) | 1.088 (1.069) | |
| | $\frac{2}{3}$ | A | 0.593 (0.881) | 0.796 (1.183) | 0.720 (1.070) | 0.720 (1.070) | 0.719 (1.068) | 0.929 (0.913) | 1.186 (1.165) | 1.088 (1.069) | 1.091 (1.072) | 1.091 (1.072) | |
| | | B | 0.386 (0.574) | 0.763 (1.134) | 0.710 (1.055) | 0.715 (1.062) | 0.719 (1.068) | -0.571 (0.561) | -1.177 (1.156) | -1.082 (1.063) | -1.088 (1.068) | -1.091 (1.072) | |
| | | C | 0.595 (0.881) | 0.351 (0.522) | 0.687 (1.021) | 0.716 (1.064) | 0.751 (1.116) | -0.929 (0.913) | -0.665 (0.653) | -1.122 (1.102) | -1.160 (1.140) | -1.187 (1.166) | |
| D | | 0.386 (0.574) | 0.867 (1.288) | 0.806 (1.198) | 0.783 (1.163) | 0.751 (1.116) | 0.571 (0.561) | 0.726 (0.713) | 1.187 (1.166) | 1.197 (1.175) | 1.187 (1.166) | | |

3. Results and discussion

3.1. CONVERGENCE OF THE RESULTS

In Fig. 1, the stress intensity factors K_{I,λ_1} and K_{II,λ_2} defined at corners A, B, C, D are analyzed with varying size, location of inclusions, and elastic ratio G_I/G_M (see Fig. 5 and Fig. 6). In the following discussion, dimensionless stress intensity factors F_{I,λ_1} and F_{II,λ_2} defined in Equation (5) are used under plane strain condition with $\nu_I = \nu_M = 0.3$.

$$F_{I,\lambda_1} = K_{I,\lambda_1}/\sigma^\infty \sqrt{\pi} l_x^{1-\lambda_1}, \quad F_{II,\lambda_2} = K_{II,\lambda_2}/\sigma^\infty \sqrt{\pi} l_x^{1-\lambda_2}. \quad (5)$$

Some examples of convergence at corner D in Fig. 3 are shown in Tables 1–3. The results shown in these tables are obtained using the boundary divisions shown in Fig. 2. In Tables 1–3, F_{I,λ_1} and F_{II,λ_2} values obtained from $W_I^I(0)$, $W_{II}^I(0)$ are indicated compared with the average

Table 11. Results for two rectangular inclusions ($G_I/G_M = 10^1$, plane strain $\nu_I = \nu_M = 0.3$)

| G_I/G_M | I_x/d_x | | $F_{I,\lambda_1} (F_{I,\lambda_1}/F_{I,\lambda_1} _{I_x \rightarrow 0})$ | | | | | $F_{II,\lambda_2} (F_{II,\lambda_2}/F_{II,\lambda_2} _{I_x \rightarrow 0})$ | | | | |
|---|-----------------|------------------|--|----------------------------------|------------------|------------------|------------------|---|----------------------------------|----------------------------------|------------------------|------------------------|
| | | | O ₁ | O ₂ | O ₃ | O ₄ | O ₅ | O ₁ | O ₂ | O ₃ | O ₄ | O ₅ |
| 10^1 $\lambda_1 = 0.7981112$ $\lambda_2 = 0.7856547$ $\alpha = -0.8181818$ $\beta = -0.2337662$ | $\rightarrow 0$ | A-D | 0.495 (1.000) | 0.495 (1.000) | 0.495 (1.000) | 0.495 (1.000) | 0.495 (1.000) | ± 0.944 (1.000) | ± 0.944 (1.000) | ± 0.944 (1.000) | ± 0.944 (1.000) | ± 0.944 (1.000) |
| | $\frac{1}{3}$ | A | 0.466 (0.941) | 0.513 (1.036) | 0.500 (1.010) | 0.499 (1.008) | 0.499 (1.008) | 0.856 (0.907) | 0.974 (1.032) | 0.954 (1.010) | 0.954 (1.010) | 0.954 (1.010) |
| | | B | 0.416 (0.840) | 0.503 (1.016) | 0.498 (1.006) | 0.498 (1.006) | 0.499 (1.008) | -0.810 (0.858) | -0.971 (1.028) | -0.953 (1.009) | -0.953 (1.010) | -0.954 (1.010) |
| | | C | 0.466 (0.941) | 0.479 (0.968) | 0.497 (1.004) | 0.499 (1.008) | 0.500 (1.010) | -0.856 (0.907) | -0.961 (1.018) | -0.957 (1.013) | -0.958 (1.015) | -0.959 (1.016) |
| | | D | 0.416 (0.840) | 0.566 (1.143) | 0.503 (1.016) | 0.502 (1.014) | 0.500 (1.010) | 0.810 (0.858) | 1.007 (1.017) | 0.959 (1.016) | 0.960 (1.017) | 0.959 (1.016) |
| | $\frac{1}{2}$ | A | 0.470 (0.949) | 0.531 (1.073) | 0.506 (1.022) | 0.503 (1.016) | 0.504 (1.018) | 0.856 (0.906) | 1.004 (1.060) | 0.964 (1.022) | 0.965 (1.022) | 0.965 (1.022) |
| | | B | 0.372 (0.752) | 0.516 (1.042) | 0.502 (1.014) | 0.503 (1.016) | 0.504 (1.018) | -0.760 (0.805) | -0.999 (1.058) | -0.963 (1.020) | -0.964 (1.022) | -0.965 (1.022) |
| | | C | 0.470 (0.949) | 0.440 (0.889) | 0.500 (1.010) | 0.505 (1.020) | 0.511 (1.032) | -0.856 (0.906) | -0.854 (0.905) | -0.977 (1.035) | -0.983 (1.042) | -0.987 (1.046) |
| | | D | 0.372 (0.752) | 0.652 (1.317) | 0.520 (1.051) | 0.516 (1.042) | 0.511 (1.032) | 0.760 (0.805) | 1.023 (1.083) | 0.986 (1.045) | 0.988 (1.047) | 0.987 (1.046) |
| | $\frac{2}{3}$ | A | 0.473 (0.956) | 0.544 (1.099) | 0.514 (1.038) | 0.514 (1.038) | 0.513 (1.036) | 0.868 (0.919) | 1.028 (1.089) | 0.980 (1.038) | 0.981 (1.040) | 0.982 (1.040) |
| | | B | 0.325 (0.657) | 0.527 (1.065) | 0.509 (1.009) | 0.511 (1.032) | 0.513 (1.036) | -0.711 (0.753) | -1.020 (1.081) | -0.978 (1.036) | -0.981 (1.039) | -0.982 (1.040) |
| | | C | 0.473 (0.956) | 0.318 (0.642) | 0.495 (1.000) | 0.511 (1.032) | 0.529 (1.069) | -0.868 (0.919) | -0.776 (0.822) | -1.009 (1.069) | -1.033 (1.094) | -1.049 (1.111) |
| | D | 0.325 (0.657) | 0.591 (1.194) | 0.561 (1.133) | 0.548 (1.107) | 0.529 (1.069) | 0.711 (0.753) | 0.711 (0.753) | 1.046 (1.108) | 1.054 (1.116) | 1.049 (1.111) | |

values. The results have good convergence, and the difference between the results and average values are within about 1%. The values obtained from $W_I^I(0)$, $W_n^I(0)$ and the average value coincide with each other in about three digits when $M = 4-6$. In the following calculation the generalized stress intensity factors are shown confirming the convergence as shown in Tables 1-3. The values of Dunders' elastic constants α , β as shown in Equation (6) are also indicated in the Tables.

$$\alpha = \frac{G_M(\kappa_I + 1) - G_I(\kappa_M + 1)}{G_M(\kappa_I + 1) + G_I(\kappa_M + 1)}, \quad \beta = \frac{G_M(\kappa_I - 1) - G_I(\kappa_M - 1)}{G_M(\kappa_I + 1) + G_I(\kappa_M + 1)}, \quad (6)$$

$$\kappa_M = 3 - 4\nu_M, \quad \kappa_I = 3 - 4\nu_I$$

Table 12. Results for two rectangular inclusions ($G_I/G_M = 2$, plane strain $\nu_I = \nu_M = 0.3$)

| G_I/G_M | I_x/d_x | | $F_{I,\lambda_1} (F_{I,\lambda_1}/F_{I,\lambda_1} _{I_x \rightarrow 0})$ | | | | | $F_{II,\lambda_2} (F_{II,\lambda_2}/F_{II,\lambda_2} _{I_x \rightarrow 0})$ | | | | | |
|---------------|-----------------|-------------------------|--|------------------|----------------|----------------|----------------|---|----------------|------------------|----------------|----------------|---------|
| | | | O ₁ | O ₂ | O ₃ | O ₄ | O ₅ | O ₁ | O ₂ | O ₃ | O ₄ | O ₅ | |
| 2 | $\rightarrow 0$ | A-D | 0.258 | 0.258 | 0.258 | 0.258 | 0.258 | ± 3.262 | ± 3.262 | ± 3.262 | ± 3.262 | ± 3.262 | |
| | | | (1.000) | (1.000) | (1.000) | (1.000) | (1.000) | (1.000) | (1.000) | (1.000) | (1.000) | (1.000) | |
| | | $\lambda_1 = 0.9109102$ | | | | | | | | | | | |
| | | $\lambda_2 = 0.9810170$ | | | | | | | | | | | |
| | $\frac{1}{3}$ | A | $\alpha = -0.3333333$ | 0.255 | 0.259 | 0.257 | 0.257 | 0.257 | 3.210 | 3.301 | 3.288 | 3.288 | 3.288 |
| | | | $\beta = -0.0952381$ | (0.988) | (1.004) | (0.996) | (0.996) | (0.996) | (0.984) | (1.012) | (1.008) | (1.008) | (1.008) |
| | | | B | 0.245 | 0.257 | 0.257 | 0.257 | 0.257 | -3.188 | -3.301 | -3.288 | -3.288 | -3.288 |
| | | | (0.950) | (0.996) | (0.996) | (0.996) | (0.996) | (0.977) | (1.012) | (1.008) | (1.008) | (1.008) | |
| | | C | | 0.255 | 0.252 | 0.257 | 0.257 | 0.257 | -3.210 | -3.293 | -3.292 | -3.294 | -3.295 |
| | | | (0.988) | (0.977) | (0.996) | (0.996) | (0.996) | (0.984) | (1.010) | (1.009) | (1.010) | (1.010) | |
| | | D | | 0.245 | 0.269 | 0.258 | 0.258 | 0.257 | 3.188 | 3.330 | 3.294 | 3.295 | 3.295 |
| | | | (0.950) | (1.042) | (1.000) | (1.000) | (0.996) | (0.977) | (1.021) | (1.010) | (1.010) | (1.010) | |
| $\frac{1}{2}$ | A | | 0.258 | 0.261 | 0.258 | 0.258 | 0.258 | 3.205 | 3.319 | 3.295 | 3.296 | 3.296 | |
| | | (1.000) | (1.012) | (1.000) | (1.000) | (1.000) | (0.983) | (1.017) | (1.010) | (1.010) | (1.010) | | |
| | | B | 0.237 | 0.258 | 0.257 | 0.257 | 0.258 | -3.166 | -3.321 | -3.295 | -3.296 | -3.296 | |
| | | (0.919) | (1.000) | (0.996) | (0.996) | (1.000) | (0.971) | (1.018) | (1.010) | (1.010) | (1.010) | | |
| | C | | 0.258 | 0.246 | 0.256 | 0.257 | 0.258 | -3.205 | -3.200 | -3.312 | -3.318 | -3.322 | |
| | | (1.000) | (0.953) | (0.992) | (0.996) | (1.000) | (0.983) | (0.981) | (1.015) | (1.017) | (1.018) | | |
| | D | | 0.237 | 0.274 | 0.260 | 0.259 | 0.258 | 3.166 | 3.249 | 3.319 | 3.322 | 3.322 | |
| | | (0.919) | (1.062) | (1.008) | (1.004) | (1.000) | (0.971) | (0.996) | (1.017) | (1.018) | (1.018) | | |
| $\frac{2}{3}$ | A | | 0.260 | 0.263 | 0.259 | 0.259 | 0.258 | 3.208 | 3.337 | 3.305 | 3.306 | 3.306 | |
| | | (1.008) | (1.019) | (1.004) | (1.004) | (1.000) | (0.983) | (1.023) | (1.013) | (1.013) | (1.013) | | |
| | | B | 0.227 | 0.259 | 0.258 | 0.258 | 0.258 | -3.145 | -3.340 | -3.305 | -3.306 | -3.306 | |
| | | (0.880) | (1.004) | (1.000) | (1.000) | (1.000) | (0.964) | (1.024) | (1.013) | (1.013) | (1.013) | | |
| | C | | 0.260 | 0.225 | 0.254 | 0.257 | 0.260 | -3.208 | -3.093 | -3.342 | -3.367 | -3.384 | |
| | | (1.008) | (0.872) | (0.984) | (0.996) | (1.008) | (0.983) | (0.948) | (1.024) | (1.032) | (1.037) | | |
| | D | | 0.227 | 0.261 | 0.267 | 0.264 | 0.260 | 3.145 | 2.973 | 3.377 | 3.388 | 3.384 | |
| | | (0.880) | (1.008) | (1.035) | (1.023) | (1.008) | (0.964) | (0.911) | (1.035) | (1.039) | (1.037) | | |

3.2. RESULTS OF SINGLE RECTANGULAR AND CYLINDRICAL INCLUSIONS

Table 4 and Fig. 3 shows the results of 2D single rectangular inclusion under longitudinal tension. The results obtained by Chen (1992) are in good agreement with the present results. Table 5 and Fig. 4 shows the results of 3D single cylindrical inclusion under longitudinal tension. The 3D results are obtained in a similar way (Noda et al., 1998b). From the comparison between 2D and 3D results we can see 2D rectangular model has a similar tendency of 3D model and looks useful as a model of real fibers.

3.3. RESULTS OF INTERACTION BETWEEN TWO SQUARE INCLUSIONS

Tables 6–9 show the intensity factors of two square inclusions at corners A, B, C, D on inclusion 1. As shown in Fig. 5, the location of inclusion 1 is changed from O₁ to O₅, the size of

Table 13. Results for two rectangular inclusions ($G_I/G_M = 10^1$, plane strain $\nu_I = \nu_M = 0.3$)

| G_I/G_M | l_x/d_x | | $F_{I,\lambda_1} (F_{I,\lambda_1}/F_{I,\lambda_1} _{l_x \rightarrow 0})$ | | | | | $F_{II,\lambda_2} (F_{II,\lambda_2}/F_{II,\lambda_2} _{l_x \rightarrow 0})$ | | | | | |
|--|-----------------|---------------|--|-------------------------|------------------|------------------|------------------|---|-------------------------|------------------------|------------------------|------------------------|------------------|
| | | | O ₁ | O ₂ | O ₃ | O ₄ | O ₅ | O ₁ | O ₂ | O ₃ | O ₄ | O ₅ | |
| 10^{-1} $\lambda_1 = 0.6601418$ $\lambda_2 = 0.9355639$ $\alpha = 0.8181818$ $\beta = 0.2337662$ | $\rightarrow 0$ | A-D | 0.351 (1.000) | 0.351 (1.000) | 0.351 (1.000) | 0.351 (1.000) | 0.351 (1.000) | ± 2.135 (1.000) | ± 2.135 (1.000) | ± 2.135 (1.000) | ± 2.135 (1.000) | ± 2.135 (1.000) | |
| | | $\frac{1}{2}$ | A | 0.379 (1.079) | 0.356 (1.014) | 0.351 (1.001) | 0.351 (1.000) | 0.350 (0.999) | 2.189 (1.025) | 2.129 (0.997) | 2.131 (0.998) | 2.130 (0.997) | 2.129 (0.997) |
| | | | B | 0.347 (0.990) | 0.342 (0.975) | 0.349 (0.996) | 0.350 (0.997) | 0.350 (0.999) | 2.165 (1.014) | 2.111 (0.989) | 2.128 (0.997) | 2.129 (0.997) | 2.129 (0.997) |
| | | | C | 0.379 (1.079) | 0.318 (0.906) | 0.347 (0.990) | 0.348 (0.993) | 0.349 (0.996) | 2.189 (1.025) | 2.122 (0.994) | 2.123 (0.994) | 2.122 (0.994) | 2.122 (0.994) |
| | D | | 0.347 (0.990) | 0.370 (1.054) | 0.351 (1.002) | 0.350 (0.999) | 0.349 (0.996) | 2.165 (1.014) | 2.118 (0.992) | 2.124 (0.994) | 2.123 (0.994) | 2.122 (0.994) | |
| | $\frac{2}{3}$ | A | 0.398 (1.134) | 0.363 (1.036) | 0.352 (1.003) | 0.351 (1.000) | 0.350 (0.997) | 2.216 (1.038) | 2.131 (1.012) | 2.126 (0.996) | 2.124 (0.995) | 2.123 (0.994) | |
| | | B | 0.323 (0.919) | 0.330 (0.940) | 0.348 (0.991) | 0.349 (0.994) | 0.350 (0.997) | 2.147 (1.006) | 2.084 (0.976) | 2.121 (0.993) | 2.122 (0.994) | 2.123 (0.994) | |
| | | C | 0.398 (1.134) | 0.347 (0.988) | 0.340 (0.968) | 0.342 (0.976) | 0.346 (0.986) | 2.216 (1.038) | 2.179 (1.020) | 2.100 (0.984) | 2.095 (0.981) | 2.093 (0.980) | |
| | | D | 0.323 (0.919) | 0.399 (1.136) | 0.353 (1.006) | 0.350 (0.996) | 0.346 (0.986) | 2.147 (1.006) | 2.356 (1.103) | 2.102 (0.984) | 2.096 (0.981) | 2.093 (0.980) | |

inclusion is changed as $l_x/d_x = \frac{1}{3}, \frac{1}{2}, \frac{2}{3}$, and the elastic ratio is changed from $G_I/G_M = 10^{-5}$ – 10^2 . The maximum stress intensity factors $F_{I,\lambda_1}, F_{II,\lambda_2}$ are indicated in **shadow**. In those tables, the ratio of the stress intensity factors to the single inclusion are also shown in the parentheses. From those tables, we can see the following.

(1) For any G_I/G_M , maximum F_{I,λ_1} values appear at the corner D when the location of inclusion 1 is on O₄, that is, when the inclusion 1 is a bit transversely shifted from the position just above inclusion 2.

(2) When $G_I/G_M > 1$, maximum F_{II,λ_2} values appear when inclusion 1 is on O₅ or O₄. When $G_I/G_M < 1$, maximum F_{II,λ_2} values appear when inclusion 1 is on O₃.

Table 14. Results for two rectangular inclusions ($G_I/G_M = 10^{-2}$, plane strain $\nu_I = \nu_M = 0.3$)

| G_I/G_M | l_x/d_x | | $F_{I,\lambda_1} (F_{I,\lambda_1}/F_{I,\lambda_1} _{l_x \rightarrow 0})$ | | | | | $F_{II,\lambda_2} (F_{II,\lambda_2}/F_{II,\lambda_2} _{l_x \rightarrow 0})$ | | | | | |
|---------------|-------------------------|-------------------------|--|------------------|----------------|----------------|------------------|---|------------------|----------------|----------------|----------------|---------|
| | | | O ₁ | O ₂ | O ₃ | O ₄ | O ₅ | O ₁ | O ₂ | O ₃ | O ₄ | O ₅ | |
| 10^{-2} | $\rightarrow 0$ | A-D | 0.489 | 0.489 | 0.489 | 0.489 | 0.489 | ± 1.979 | ± 1.979 | ± 1.979 | ± 1.979 | ± 1.979 | |
| | | | (1.000) | (1.000) | (1.000) | (1.000) | (1.000) | (1.000) | (1.000) | (1.000) | (1.000) | (1.000) | |
| | | $\lambda_1 = 0.5583162$ | A | 0.550 | 0.504 | 0.491 | 0.490 | 0.489 | 2.030 | 1.981 | 1.975 | 1.973 | 1.972 |
| | | | | (1.124) | (1.029) | (1.003) | (1.001) | (0.999) | (1.026) | (1.001) | (0.998) | (0.997) | (0.997) |
| | $\lambda_2 = 0.9116800$ | B | 0.490 | 0.467 | 0.486 | 0.487 | 0.489 | 2.010 | 1.948 | 1.971 | 1.971 | 1.972 | |
| | | | (1.002) | (0.955) | (0.994) | (0.996) | (0.999) | (1.007) | (0.984) | (0.996) | (0.996) | (0.997) | |
| | $\alpha = 0.9801980$ | C | (0.550) | 0.424 | 0.483 | 0.485 | 0.487 | 2.030 | 1.964 | 1.964 | 1.964 | 1.964 | |
| | | | (1.124) | (0.866) | (0.987) | (0.991) | (0.996) | (1.026) | (0.993) | (0.993) | (0.992) | (0.993) | |
| | $\beta = 0.2800566$ | D | 0.490 | 0.528 | 0.491 | 0.489 | 0.487 | 2.010 | 1.979 | 1.968 | 1.966 | 1.964 | |
| | | | (1.002) | (1.080) | (1.004) | (1.000) | (0.996) | (1.007) | (1.000) | (0.994) | (0.993) | (0.993) | |
| | $\frac{1}{3}$ | $\frac{1}{2}$ | A | 0.585 | 0.522 | 0.494 | 0.491 | 0.488 | 2.066 | 2.008 | 1.971 | 1.968 | 1.965 |
| | | | | (1.196) | (1.066) | (1.009) | (1.004) | (0.999) | (1.044) | (1.014) | (0.996) | (0.994) | (0.993) |
| B | | | 0.444 | 0.424 | 0.483 | 0.486 | 0.488 | 1.990 | 1.912 | 1.961 | 1.963 | 1.965 | |
| | | | (0.907) | (0.866) | (0.987) | (0.993) | (0.999) | (0.990) | (0.966) | (0.991) | (0.992) | (0.993) | |
| C | | 0.585 | 0.473 | 0.469 | 0.475 | 0.482 | 2.066 | 2.044 | 1.939 | 1.934 | 1.933 | | |
| | | (1.196) | (0.967) | (0.958) | (0.971) | (0.985) | (1.044) | (1.033) | (0.980) | (0.977) | (0.977) | | |
| D | | 0.444 | 0.549 | 0.496 | 0.489 | 0.482 | 1.990 | 2.348 | 1.945 | 1.937 | 1.933 | | |
| | | (0.907) | (1.123) | (1.014) | (1.000) | (0.985) | (0.990) | (1.186) | (0.983) | (0.979) | (0.977) | | |
| $\frac{2}{3}$ | | A | 0.617 | 0.560 | 0.499 | 0.494 | 0.489 | 2.096 | 2.028 | 1.970 | 1.963 | 1.957 | |
| | | | (1.260) | (1.146) | (1.020) | (1.011) | (0.999) | (1.059) | (1.025) | (0.995) | (0.992) | (0.989) | |
| | | B | 0.382 | 0.381 | 0.477 | 0.483 | 0.489 | 1.942 | 1.845 | 1.949 | 1.952 | 1.957 | |
| | | | (0.782) | (0.779) | (0.974) | (0.986) | (0.999) | (0.981) | (0.932) | (0.985) | (0.987) | (0.989) | |
| C | 0.617 | 0.567 | 0.430 | 0.445 | 0.466 | 2.096 | 2.069 | 1.902 | 1.871 | 1.854 | | | |
| | (1.260) | (1.160) | (0.879) | (0.909) | (0.953) | (1.059) | (1.045) | (0.961) | (0.945) | (0.937) | | | |
| D | 0.382 | 0.570 | 0.511 | 0.491 | 0.466 | 1.942 | 2.660 | 1.893 | 1.862 | 1.854 | | | |
| | (0.782) | (1.166) | (1.044) | (1.003) | (0.953) | (0.981) | (1.344) | (0.956) | (0.941) | (0.937) | | | |

3.4. RESULTS OF INTERACTION BETWEEN TWO RECTANGULAR INCLUSIONS

Tables 10–15 show the intensity factors at the corners A, B, C, D on inclusion 1 when two rectangular inclusions has the same aspect ratio $l_y/l_x = 10$. As shown in Figure 6, the location of inclusion 1 is changed from O₁ to O₅, the size of inclusion is changed as $l_x/d_x = \frac{1}{3}, \frac{1}{2}, \frac{2}{3}$, and the elastic ratio is changed from $G_I/G_M = 10^{-5} \sim 10^2$. The maximum stress intensity factors F_{I,λ_1} , F_{II,λ_2} are indicated in **shadow**. In those tables, the ratio of the stress intensity factors to the single inclusion are also shown in the parentheses. From tables 9–14 we can see the following.

- (1) When $G_I/G_M > 1$ in Fig. 6:

Table 15. Results for two rectangular inclusions ($G_I/G_M = 10^{-5}$, plane strain $\nu_I = \nu_M = 0.3$)

| G_I/G_M | I_x/d_x | | $F_{I,\lambda_1} (F_{I,\lambda_1}/F_{I,\lambda_1} _{I_x \rightarrow 0})$ | | | | | $F_{II,\lambda_2} (F_{II,\lambda_2}/F_{II,\lambda_2} _{I_x \rightarrow 0})$ | | | | |
|-------------------------|-----------------|-----|--|----------------|----------------|----------------|----------------|---|------------------|----------------|----------------|----------------|
| | | | O ₁ | O ₂ | O ₃ | O ₄ | O ₅ | O ₁ | O ₂ | O ₃ | O ₄ | O ₅ |
| 10^{-5} | $\rightarrow 0$ | A-D | 0.513 | 0.513 | 0.513 | 0.513 | 0.513 | ± 1.968 | ± 1.968 | ± 1.968 | ± 1.968 | ± 1.968 |
| $\lambda_1 = 0.5444838$ | | | (1.000) | (1.000) | (1.000) | (1.000) | (1.000) | (1.000) | (1.000) | (1.000) | (1.000) | (1.000) |
| $\lambda_2 = 0.9085292$ | $\frac{1}{3}$ | A | 0.583 | 0.530 | 0.515 | 0.514 | 0.513 | 2.017 | 1.972 | 1.964 | 1.962 | 1.961 |
| $\alpha = 0.9999800$ | | | (1.135) | (1.032) | (1.004) | (1.002) | (0.999) | (1.025) | (1.002) | (0.998) | (0.997) | (0.996) |
| $\beta = 0.2857086$ | | B | 0.517 | 0.488 | 0.510 | 0.512 | 0.513 | 1.999 | 1.936 | 1.960 | 1.960 | 1.961 |
| | | | (1.008) | (0.950) | (0.994) | (0.996) | (0.999) | (1.015) | (0.983) | (0.996) | (0.996) | (0.996) |
| | | C | 0.583 | 0.440 | 0.506 | 0.509 | 0.511 | 2.017 | 1.954 | 1.953 | 1.953 | 1.953 |
| | | | (1.135) | (0.857) | (0.986) | (0.991) | (0.996) | (1.025) | (0.993) | (0.992) | (0.992) | (0.992) |
| | | D | 0.517 | 0.557 | 0.516 | 0.514 | 0.511 | 1.999 | 1.973 | 1.957 | 1.955 | 1.953 |
| | | | (1.008) | (1.084) | (1.005) | (1.001) | (0.996) | (1.015) | (1.002) | (0.994) | (0.993) | (0.992) |
| | $\frac{1}{2}$ | A | 0.621 | 0.547 | 0.519 | 0.516 | 0.513 | 2.054 | 2.008 | 1.960 | 1.957 | 1.954 |
| | | | (1.211) | (1.066) | (1.010) | (1.005) | (0.999) | (1.044) | (1.020) | (0.996) | (0.994) | (0.993) |
| | | B | 0.466 | 0.431 | 0.506 | 0.510 | 0.513 | 1.976 | 1.902 | 1.950 | 1.951 | 1.954 |
| | | | (0.908) | (0.840) | (0.986) | (0.992) | (0.999) | (1.004) | (0.966) | (0.991) | (0.991) | (0.993) |
| | | C | 0.621 | 0.491 | 0.491 | 0.498 | 0.506 | 2.054 | 2.047 | 1.927 | 1.922 | 1.921 |
| | | | (1.211) | (0.956) | (0.956) | (0.970) | (0.986) | (1.044) | (1.040) | (0.979) | (0.977) | (0.976) |
| | | D | 0.466 | 0.563 | 0.521 | 0.514 | 0.506 | 1.976 | 2.384 | 1.934 | 1.926 | 1.921 |
| | | | (0.908) | (1.096) | (1.015) | (1.001) | (0.986) | (1.004) | (1.211) | (0.983) | (0.978) | (0.976) |
| | $\frac{2}{3}$ | A | 0.656 | 0.593 | 0.525 | 0.520 | 0.514 | 2.086 | 2.031 | 1.960 | 1.953 | 1.946 |
| | | | (1.278) | (1.156) | (1.023) | (1.013) | (1.000) | (1.060) | (1.032) | (0.996) | (0.992) | (0.989) |
| | | B | 0.398 | 0.382 | 0.499 | 0.506 | 0.514 | 1.930 | 1.829 | 1.937 | 1.940 | 1.946 |
| | | | (0.774) | (0.745) | (0.972) | (0.986) | (1.000) | (0.981) | (0.929) | (0.984) | (0.986) | (0.989) |
| | | C | 0.656 | 0.609 | 0.448 | 0.465 | 0.490 | 2.086 | 2.048 | 1.890 | 1.858 | 1.841 |
| | | | (1.278) | (1.187) | (0.873) | (0.906) | (0.954) | (1.060) | (1.040) | (0.960) | (0.944) | (0.936) |
| | | D | 0.398 | 0.630 | 0.539 | 0.516 | 0.490 | 1.930 | 2.672 | 1.882 | 1.850 | 1.841 |
| | | | (0.774) | (1.228) | (1.049) | (1.006) | (0.954) | (0.981) | (1.353) | (0.956) | (0.940) | (0.936) |

(a) Stress intensity factors F_{I,λ_1} , F_{II,λ_2} appear larger than the ones of a single inclusion when inclusion 1 is on O₃, O₄, O₅, that is, when two inclusion are in longitudinal tensile direction.

(b) Stress intensity factors F_{I,λ_1} , F_{II,λ_2} appear smaller than the ones of a single inclusion when inclusion 1 is on O₁, that is, when two inclusion are in transverse direction.

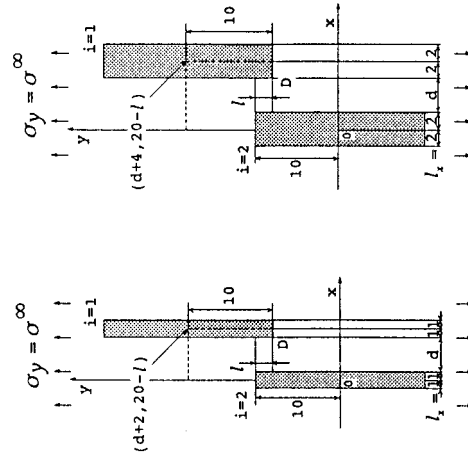
(c) Stress intensity factors F_{I,λ_1} , F_{II,λ_2} appear largest when inclusion 1 is on O₂, that is, when the two inclusions are in the skew direction. Within the analysis in this paper the maximum interaction appears +51%.

(2) When $G_I/G_M < 1$ in Fig. 6:

(d) Stress intensity factors F_{I,λ_1} , F_{II,λ_2} appear smaller than the ones of a single inclusion when inclusion 1 is on O₃, O₄, O₅, that is, when two inclusion are almost in longitudinal tensile direction.

Table 16. Comparison between the results $l_x = 1$ and $l_x = 2$ ($F_{1,\lambda_1}^* = K_{1,\lambda_1}/\sigma^\infty \sqrt{\pi}$, $F_{11,\lambda}^* = K_{11,\lambda_2}/\sigma^\infty \sqrt{\pi}$, $G_I/G_M = 10^2$, Plane strain $\nu_I = \nu_M = 0.3$)

| l | l_x/d | F_{1,λ_1}^* | | | | | F_{11,λ_2}^* | | | | |
|-----|---------|---------------------|-------|-------|-------|-------|----------------------|-------|-------|-------|-------|
| | | 1 | 2 | 3 | 4 | 5 | 1 | 2 | 3 | 4 | 5 |
| 0 | 1 | 1.013 | 0.775 | 0.686 | 0.644 | 0.624 | 1.292 | 1.089 | 1.014 | 0.983 | 0.971 |
| | 2 | 0.956 | 0.706 | 0.609 | 0.562 | 0.539 | 1.306 | 1.093 | 1.015 | 0.981 | 0.967 |
| 1 | 1 | 0.921 | 0.715 | 0.642 | 0.612 | 0.602 | 1.198 | 1.052 | 0.992 | 0.970 | 0.965 |
| | 2 | 0.878 | 0.647 | 0.563 | 0.528 | 0.514 | 1.245 | 1.071 | 1.002 | 0.973 | 0.963 |
| 10 | 1 | 0.456 | 0.529 | 0.576 | 0.609 | 0.632 | 0.654 | 0.754 | 0.815 | 0.863 | 0.900 |
| | 2 | 0.396 | 0.474 | 0.520 | 0.549 | 0.568 | 0.561 | 0.650 | 0.720 | 0.780 | 0.830 |



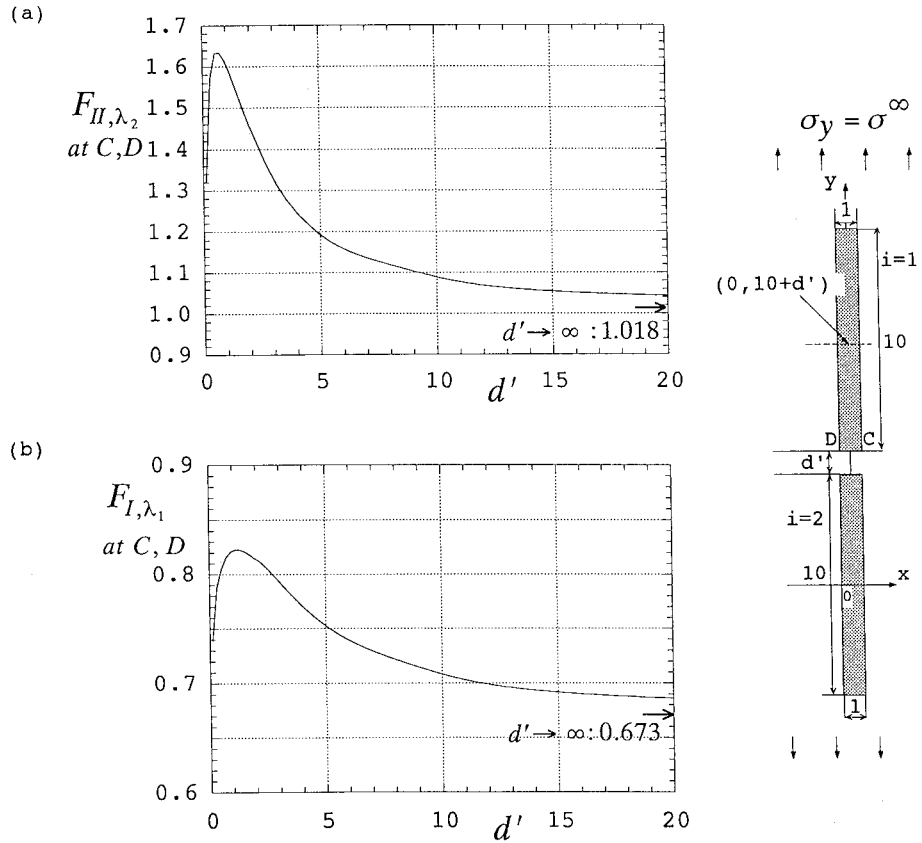


Figure 8. (a) F_{I, λ_1} at D vs. d' relation (b) F_{II, λ_2} at D vs. d' relation ($G_I/G_M = 10^2$, Plane strain $\nu_I = \nu_M = 0.3$).

4. Conclusions

In this paper, an interaction between two rectangular inclusions under longitudinal tension as shown in Figure 1 is considered. Generalized stress intensity factors at the corners of inclusions were discussed and tabulated for various geometrical conditions and elastic ratios. The conclusions can be made as follows.

(1) In the numerical solution of the singular integral equations of the body force method, the unknown body force densities are approximated by piecewise smooth functions using power series and two types of fundamental density functions. The calculation shows that the present method yields rapidly converging results for the wide range of geometrical and elastic conditions.

(2) When $G_I/G_M > 1$ in Figure 6:

(a) Stress intensity factors F_{I, λ_1} , F_{II, λ_2} appear larger than the ones of a single inclusion when inclusion 1 is on O_3 , O_4 , O_5 , that is, when two inclusions are in longitudinal tensile direction.

(b) Stress intensity factors F_{I, λ_1} , F_{II, λ_2} appear smaller than the ones of a single inclusion when inclusion 1 is on O_1 , that is, when two inclusions are in transverse direction.

(c) Stress intensity factors F_{I,λ_1} , F_{II,λ_2} appear largest when inclusion 1 is on O_2 , that is, when two inclusions are in the skew direction. Within the analysis in this paper the maximum interaction appears +51%.

(3) When $G_I/G_M < 1$ in Figure 6:

(d) Stress intensity factors F_{I,λ_1} , F_{II,λ_2} appear smaller than the ones of a single inclusion when inclusion 1 is on O_3 , O_4 , O_5 , that is, when two inclusions are in the longitudinal tensile direction.

(e) Stress intensity factors F_{I,λ_1} , F_{II,λ_2} appear largest when inclusion 1 is on O_1 or O_2 , that is, when the two inclusions are in transverse or skew direction. Within the analysis in this paper the maximum interaction appears 35%.

(4) Stress intensity factors are investigated in detail when two rectangular inclusions become closer and $G_I/G_M > 1$.

(a) If the two inclusions are situated in the skew-direction, the stress intensity factors F_{I,λ_1} and F_{II,λ_2} increase significantly with decreasing the x -distance d .

(b) If the two inclusions are situated in the x -direction, F_{I,λ_1} and F_{II,λ_2} decrease as $d \rightarrow 0$.

(c) If the two inclusions are situated in the y -direction, F_{I,λ_1} and F_{II,λ_2} increase until the peak values near $d' = 0$ and finally decrease with decreasing the y -distance between the two inclusions.

Acknowledgements

This research was supported by Kyushu Institute of Technology Fellowship for Foreign Researchers in 1998. The authors wish to express their thanks to the members of their group, especially Mr T. Imahashi and Mr Y. Okuda, who carried out much of the constructional work.

References

- Bogy, D.B. and Wang, K.C. (1971). Stress singularities at interface corners in bonded dissimilar isotropic elastic materials. *International Journal of Solids and Structures*, **7**, 993–1005.
- Chen, D.H. (1992). Analysis for corner singularity in composite materials based on the body force method. *Localized Damage II* **1**, 397–421.
- Chen, D.H. and Nisitani, H. (1993). Singular stress near the corner of jointed dissimilar materials. *ASME Journal of Applied Mechanics* **60**, 607–613.
- Nisitani, H. (1967). The two-dimensional stress problem solved using an electric digital computer. *Journal of the Japan Society of Mechanical Engineers* **70**, 627–632. [*Bulletin of Japan Society of Mechanical Engineers* **11** (1968), 14–23.]
- Noda, N.-A. and Matsuo, T. (1998). Singular integral equation method for interaction between elliptical inclusions. *ASME Journal of Applied Mechanics* **65**, 310–319.
- Noda, N.-A., Kawashima, Y., Moriyama, S., and Oda, K., (1996). Interaction of newly defined stress intensity factors for angular corners in a row of diamond-shaped inclusions. *International Journal of Fracture* **82**, 267–295.
- Noda, N.-A., Wang, Q., Uemura, Y., and Kawashima, Y., (1998a). Singular integral equation method in the analysis of interaction between rectangular inclusion. *JSME International Journal* **A41**(3), 303–308.
- Noda, N.-A., Wang, Q., Morodomi, T., and Uemura, Y., (1998b). Analysis of newly defined stress intensity factors at the end of rectangular and cylindrical inclusions. *Key Engineering Materials* **145–149**, 77–82.